International Journal of Industrial Electronics, Control and Optimization © 2018 IECO

Vol. 1, No. 1, pp. 71-80, June (2018)

Torque Ripple Minimization in SRM Based on Advanced Torque Sharing Function Modified by Genetic Algorithm Combined with Fuzzy PSO

Hassan Moradi CheshmehBeigi[a] and **Alireza Mohamadi Amidi**[b]

ABSTRACT

This paper presents a new and improved Torque Sharing Function (TSF) to minimize torque ripple of Switched Reluctance Motor (SRM). This approach combined of three steps. At first step, Genetic Algorithm has been used to define the best Turn-on and Turn-off angel of phase current. At second step, a fuzzy logic controller system has been designed as a new TSF. Finally, at the last step, Particle Swarm Optimization (PSO) has been used to optimize Fuzzy membership function. The two main merits of this approach are that the proposed control algorithm can be used in wide speed ranges and also three-step-design and optimization makes this approach enable to perfectly results in smooth torque. The effectiveness of this approach has been verified through a simulation of four phase 8/6 SRM in Matlab/Simulink. Obtained result from simulation shown that the produced torque was high quality and its ripple was one-third of fuzzy TSF. This proposed method is very powerful to adapt itself for various kind of SRMs with different parameters.

ARTICLE INFO

Keywords:
SRM
Torque Sharing Function
Ripple Minimization
Fuzzy Interface System
Article history:
Received March. 7, 2018
Accepted May. 1, 2018

I. INTRODUCTION

Switched Reluctance Motors (SRM) has gained attention from industry and researchers due to its simple structure, lack of use of magnet or winding on rotor, high power density, and low operation cost[1]. However, due to salient pole of stator and rotor, SRM have the problem of high torque ripple[2]. When a pole is transferring from one phase to another phase, a big torque ripple occurs which makes oscillation in rotor speed and a big sound noise. Usually, there are two main approaches in regard to the ripple minimization of SRM. The first approach is a proper mechanical design of rotor and stator, and the second approach is the control method[3]. In[4] and[5], mechanical design has been combined with control approach to reduce torque ripple and produce constant torque.

One of the most convenient approach to reduce torque ripple is to share torque of incoming phase and outgoing phase. This approach is called Torque Sharing Function (TSF). TSF defines a torque shape in overlap area of incoming and outgoing phase, and the phase should produce the referenced torque assigned by the TSF. Some of the primary approaches of TSF are linear, cubic, cosine, and exponential type of TSF used in the literature[6]. However, these TSF implementation are very simple, but they do not improve torque profile so much. In[7], an optimization algorithm is used to minimize torque ripple. In[8], an online logical TSF is introduced to improve torque profile. This is claimed the logical TSF changes according to the situation. However, flux range change in this approach is very high and the stator loss is a lot.

Due to the nonlinearity of SRM,[9] and[10] proposed an iterative learning approach to minimize torque ripple. Ref[11] presents a novel DTC strategy for a six-phase transverse flux permanent magnet motor. Ref[12] introduces a novel magnetically isolated phase structure for switched reluctance motor, namely, as SeptiSegment SRM, which is proper for high torque/volume and with lowest leakage flux in different fields of industries. In[13], a fuzzy TSF has been proposed to control phase torque. This approach has been tested on a 12/8 SRM, but the result is not that good in motor with lower rotor/stator pole.

This paper presents an improved TSF approach in which Genetic Algorithm (GA) defines Turn-on and Turn-off angles of phases and the size of overlap area and fuzzy logic controller defines rising and falling shape of TSF. Also, to improve torque sharing function, PSO algorithm is applied to optimize fuzzy membership functions. This approach not only works very well in entire speed of range, but also give a lower torque ripple in comparison with other techniques. The paper presented as follows; the second section provides an explanation on the SRM mechanism and TSF. The Third section gives a brief illustration on FLC, GA, and PSO. Section four gives the results and the final section concludes the paper.

[a] Corresponding Author: Ha.moradi@razi.ac.ir, Tel: +98-833-4274530, Fax: +98-833-4274542, Electrical Engineering, Razi University, Kermanshah, Iran
[b] Electrical Engineering, Razi University, Kermanshah, Iran
http://dx.doi.org/10.22111/ieco.2018.24302.1016

II. TORQUE SHARING FUNCTION IN SRM

A. Switched Reluctance motor

In SRM, each stator phase has two series windings to produce magnetic flux. Change in magnetic path causes the rotor to turn. Equation for kth phase is as follows[14]:

$$v_k = R_s i_k + \frac{d\lambda_k(\theta_r \cdot i)}{dr} \tag{1}$$

in Eq. (1), linkage flux of each phase is $\lambda_k(\theta_r \cdot i) = L(\theta_r i) i_k$. So we have:

$$v_k = R_s i_k + L(\theta_r \cdot i)\frac{di_k}{dr} + \frac{dL(\theta_r \cdot i)}{d\theta_r}\omega_r i_k \tag{2}$$

where ω_r is angular speed of the rotor. In a linear magnetic area, co-energy can be defined as follows:

$$W_c = \int \lambda di \tag{3}$$

$$T(i \cdot \theta) = \frac{\partial W_c}{\partial \theta} = \frac{\partial}{\partial \theta}\int_0^t \lambda di \tag{4}$$

Eq. (4) can be written as follows[15]:

$$T(i \cdot \theta) = \frac{1}{2} i^2 \frac{dL}{d\theta} \tag{5}$$

Eq. (5) shows that instantaneous torque is proportional to the square of current and instantaneous change of inductance. Also, the total instantaneous torque of a SRM is achieved by sum of each phase torques:

$$T_e = \sum_{k=1}^{m} T_k(i \cdot \theta) \tag{6}$$

According to the Fig. 1, when inductance slop is positive and there is a current in the related phase, a positive torque is produced and when the slope is zero, the output torque is zero. Also, when the slope is negative, phase current should be zero, otherwise it produces negative torque. Four distinct induction regions emerge is given in Table I.

B. TORQUE SHARING FUNCTION

In this paper, TSF control structure is used to share torque between commutation intervals. A constant torque can be produced if torque sharing between incoming and outgoing phase is well introduced. Due to the lack of torque during commutation interval, TSF can be used to keep the produced torque constant. The design of TSF is very important, otherwise it can result is higher torque ripple. The proper sharing of torque can remove torque ripple in SRM. So, torque request should be distributed between two phases[16]. The torque can be written as a sum of two phases such x and y:

$$T_e^* = T_x^* + T_y^* \tag{7}$$

where:

$$T_x^* = T_e^* * f_x(\theta) \tag{8}$$

$$T_y^* = T_e^* * f_y(\theta) \tag{9}$$

where $f_x(\theta)$ and $f_y(\theta)$ are the x and y TSF. In commutation interval θ_i is start angel and θ_f is final angle for commutation interval. For instance, for a four phase 8/6 SRM, we have:

$$15^\circ > \theta_f > \theta_i \geq 0^\circ \tag{10}$$

In[17], a cosine TSF was proposed which f_x and f_y functions are as follows:

$$f_x(\theta) = \begin{cases} 1 & for \quad 0^\circ \leq \theta \leq \theta_i \\ \dfrac{1 + cosk(\theta - \theta_i)}{2} & for \quad \theta_i \leq \theta \leq \theta_f \\ 0 & for \quad \theta_f \leq \theta \leq 15^\circ \end{cases} \tag{11}$$

$$f_y(\theta) = \begin{cases} 0 & for \quad 0^\circ \leq \theta \leq \theta_i \\ \dfrac{1 + cosk(\theta - \theta_i)}{2} & for \quad \theta_i \leq \theta \leq \theta_f \\ 1 & for \quad \theta_f \leq \theta \leq 15^\circ \end{cases} \tag{12}$$

where:

$$k = \frac{180}{\theta_f - \theta_i} \tag{13}$$

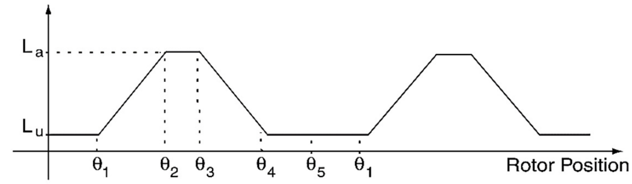

FIG. 1. Inductance change according to the rotor position.

TABLE I. Four distinct induction regions emerge

Angeles	Region
$\theta - \theta_1$	No Overlapping
$\theta_1 - \theta_2$	Poles Overlapping
$\theta_2 - \theta_3$	Complete Overlapping
$\theta_3 - \theta_4$	Partial Overlapping
$\theta_4 - \theta_5$	No Overlapping

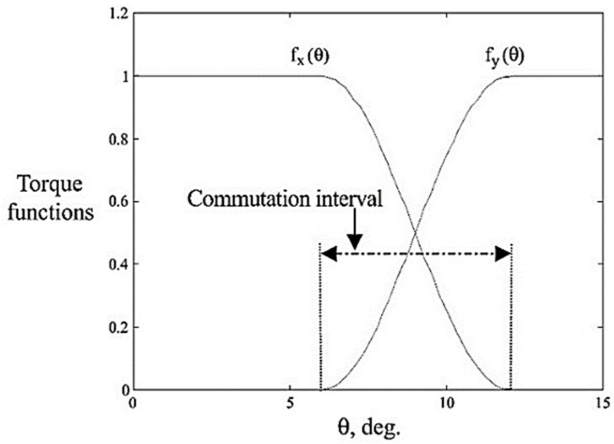

FIG. 2. Cosine TSF[14].

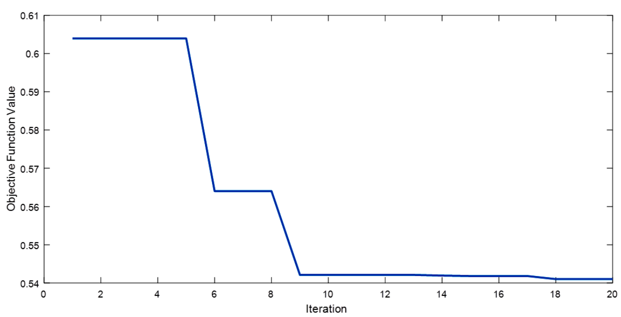

FIG. 3. GA convergence for tuning the best angles.

The TSF schematic is illustrated in Fig. 2. It should be mentioned that rising and falling shape of Fig. 2 is going to be replaced by FIS. There are two fuzzy systems, which one of them is for rising part of incoming phase and the second fuzzy is for falling part ofoutgoing phase.

III. PROPOSED METHODS

In this section, GA, Fuzzy Interface System and PSO algorithm are explained in summery.

A. GENETIC ALGORITHM

GA is an evolutionary algorithm inspired by natural selection[18]. The algorithm repeatedly modifies its population base on three main process. The first process is named selection, by which two parents are chosen to breed a new generation. This selection is upon on a fitness-based process. In the second step, crossover is done to change the programing of the chromosome. In the third part, mutation is done to keep genetic diversity[19].

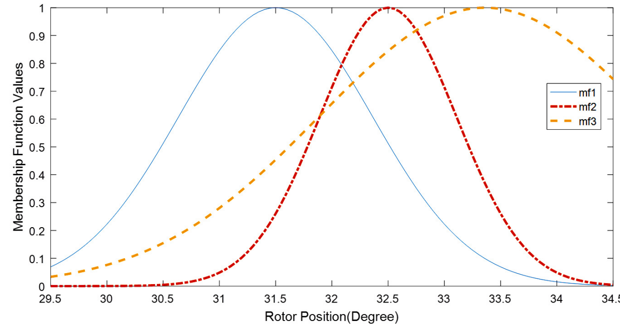

FIG. 4. Input membership function for rising FIS.

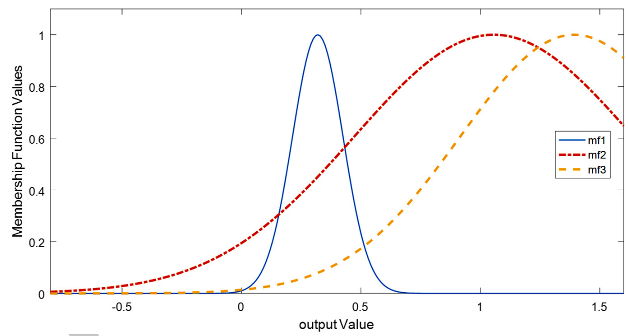

FIG. 5. Output membership function for rising FIS.

B. FUZZY INTERFACE SYSTEM

Fuzzy inference is the process of formulating the mapping from a given input to an output using fuzzy logic. It was introduced by Lotfi Zadeh in 1973[20]. Fuzzy inference system includes 4 important parts including fuzzification, membership function, if-then rules and fuzzy logic operators, and defuzzification. There exist two types of fuzzy inference system i.e. Mamdanis fuzzy inference method[21] and Sugeno-type fuzzy inference system[22]. Mamdani's method is the most popular fuzzy method. It was proposed in 1975 by Ebrahim Mamdani as an attempt to control the flow of steam engine and boiler by creating a set of linguistic control rules obtained from experienced human operators[23]. In this paper, the researchers knowledge has been used to build the initial fuzzy and then, PSO has been applied to optimized fuzzy membership functions.

1. MEMBERSHIP FUNCTION

There exist two fuzzy interface systems for this research. According to Fig. 2, one of them is rising part of commutation interval, which is reference for incoming phase, and the second one is falling part which is for outgoing part. So, two FISs i.e. rising FIS and falling FIS are designed to form TSF. Rising FIS has one input and one output. The input gets rotor position angle and the output gives rising part of TSF. Also, the falling FIS

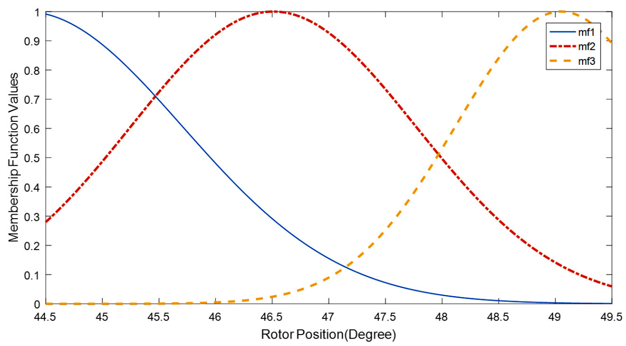

FIG. 6. Input membership function for falling FIS.

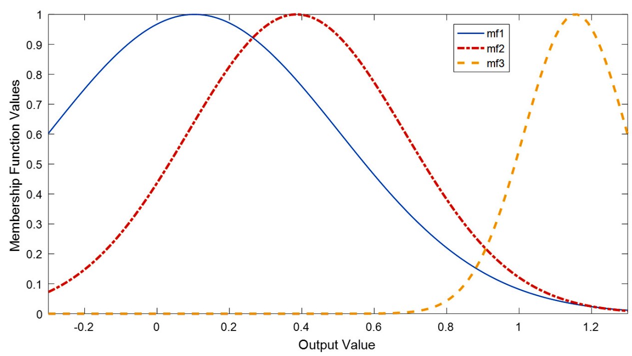

FIG. 7. Output membership function for falling FIS.

has one input and one output. GA has been used to define the best starting and ending fire angle of the phases. The best turn-on angel for the 8/6 SRM, which has been used here, is 32° and the best turn-off angel is 47°. GA determines 5° as a best commutation interval. GA convergence is depicted in Fig. 3. GA calculates these angles base on the fact that the torque ripple is kept in lowest value. So for the rising FIS, the membership functions of input and output are depicted in Fig. 4 and Fig. 5, respectively. Also, for the falling FIS, the membership functions of input and output are depicted in Fig. 6 and Fig. 7, respectively. The above-mentioned membership functions and their rules are designed so that the initial behavior of FIS follow the FIS behavior of Ref[13]. Then they will be upgraded and optimized.

2. FUZZY RULES

Falling and rising FIS has different rules, and the rules have been defined based on authors experience. The rules of rising FIS is given in Table II. As the rotor approaches the incoming phase, the rules and membership values for rising FIS gains importance and the authors define more rules when rotor is closing to the phase. The rules of falling FIS is given in Table III. In the falling FIS, the authors define more rules in middle and end of commutation interval since falling FIS value in this region is more important.

TABLE II. Rising FIS rules

Rules Number	Input MF Name	Output MF Name	Rule Weight
1	Mf1	Mf2	1
2	Mf2	Mf1	1
3	Mf3	Mf3	1
4	Mf3	Mf2	0.4
5	Mf3	Mf1	0.5

TABLE III. Falling FIS rules

Rules Number	Input MF Name	Output MF Name	Rule Weight
1	Mf1	Mf3	1
2	Mf2	Mf2	1
3	Mf3	Mf1	1
4	Mf2	Mf3	1

C. PARTICLE SWARM OPTIMIZATION

The PSO is chosen as optimization algorithm since its results are so accurate and does not need complex calculation[24,19]. Also base on previous works on fuzzy optimization, PSO can optimize fuzzy membership function more accurately and quickly in comparison to other algorithms[25]. Different literature is explained PSO in detail[26,27].

In the basic PSO technique, suppose that the search space is d-dimensional,

1. Each member is called particle, and each particle (i-th particle) is represented by d-dimensional vector and described as $X_i = [x_{i1}, x_{i2}, \cdots, x_{id}]$.

2. The set of n particle in the swarm are called *population* and described as $pop = [x_1, x_2, \cdots, x_n]$.

3. The best previous position for each particle (the position giving the best fitness value) is called *particle best* and described as $PB_i = [pb_{i1}, pb_{i2}, \cdots, pb_{id}]$.

4. The best position among all of the particle best position achieved so far is called *global best* and described as $GB = [gb_1, gb_2, \cdots, gb_d]$.

5. The rate of position change for each particle is called *the particle velocity* and described as $V_i = [v_{i1}, v_{i2}, \cdots, v_{id}]$.
   At iteration k the velocity for d-dimension of i-particle is updated by:

$$v_{id}^{k+1} = wv_{id}^{k} + c_1 r_1 (pb_{id}^{k} - X_{id}^{k}) + c_2 r_2 (gb_{d}^{k} - X_{id}^{k}) \quad (14)$$

where $i = 1, 2, \cdots, n$ and n is the size of population, w is the inertia weight, c_1 and c_2 are the acceleration constants, and r_1 and r_2 are two random values in range $[0, 1]$.

6. The i-particle position is updated by

$$X_{id}^{k+1} = X_{id}^{k} + V_{id}^{k+1} \tag{15}$$

Flow chart of optimization is shown in Fig. 8.
The flowchart works as follows:

1. PSO parameters are determined
2. Boundaries of center and sigma of membership functions are defined.
3. The Fuzzy Inference System (FIS) is initialized.
4. PSO updates its positions and velocities.
5. PSO runs MATLAB/Simulink and provide it with a new FISs. After simulation, PSO calculates the objective function value.
6. If this new FIS results in a better answer, it is considered as a best FIS up to now.
7. If stop condition is not met, go to step 4.
8. Print the results.

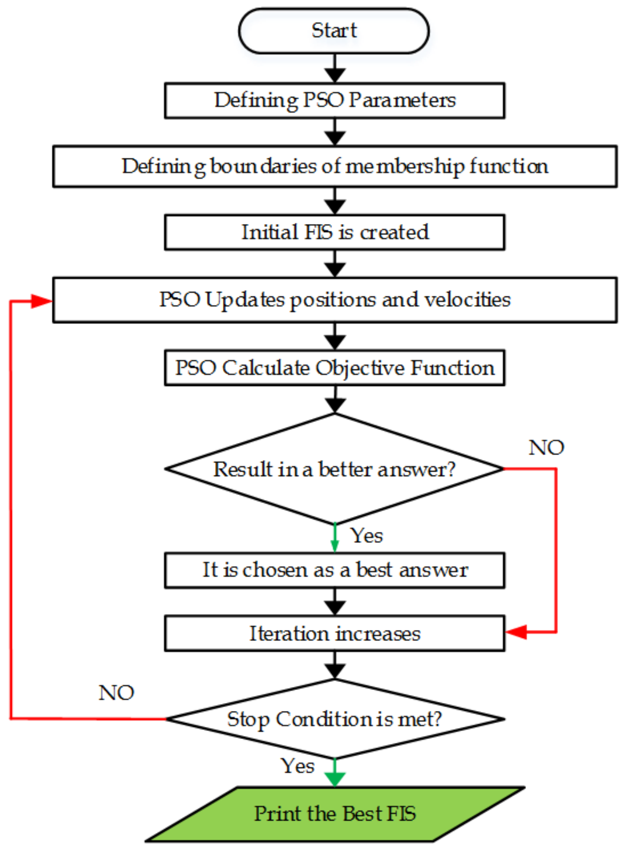

FIG. 8. Optimization flowchart.

D. CONTROL STRUCTURE

Control structure used in this paper is shown in Fig. 9. There is a PI controller to track reference speed by defining torque reference. Torque is mapped by a lookup table to current reference. Also, there is an encoder to determine rotor position. $\square_{\text{on}}$ and $\square_{\text{off}}$ and rotor position are provided to the TSF box to determine reference shape. TSF box can be a simple shape with no overlap, a Cos TSF, Fuzzy TSF, and optimized Fuzzy TSF. The current refe rence is then achieved by multiplying the current reference value in TSF shape. A hysteresis controller is also used to track the current by turning on and off the IGBTs of converter.

IV. FUZZY TRAINING AND NUMERICAL STUDY

To validate the proposed method, the system has been simulated in Matlab/Simulink. Also, Matlab/mfile has been used to execute code for PSO, GA, and FIS. A four phase 8/6 SRM is used to validate the results. Motor parameters are given in Table IV. To compare the effectiveness of the proposed method, the results have been compared with a Cosine TSF[17] and a Fuzzy Logic Controller designed in[13]. The following is divided into two parts. In the first part, PSO has been employed to tune fuzzy membership functions of both the rising and falling FIS, and in the second part, the results of proposed method are compared to results of two papers.

TABLE IV. Motor parameters

Dc-Link Voltage	300 V
Stator Resistance	0.05 Ω
Inductance L_{min}	0.1 mH
Inductance L_{max}	0.5 mH
Stator Pole Number	8
Rotor Pole Number	6

A. FUZZY TRAINING USING PSO

In this part, PSO has been employed to train rising and falling FIS for torque sharing function. It is worth to mentioned that, as shown in Fig. 2, there exist three part i.e. rising part, constant part, and falling part. In this paper, the authors not only changed the rising and falling part by defining new FIS, but also the area in which the reference torque was constant has changed as well. It is considered somehow increasing as. The reason behind this alteration is that, as the rotor is entered to the phase arc, if the flux is slowly increased, the torque can be increased so that the lack of torque between commutations can be decreased. This increase in constant part of Fig. 2 is done base on different trial and error simulations. So instead of considering a constant value of K in this interval, Eq. (16) has been considered for

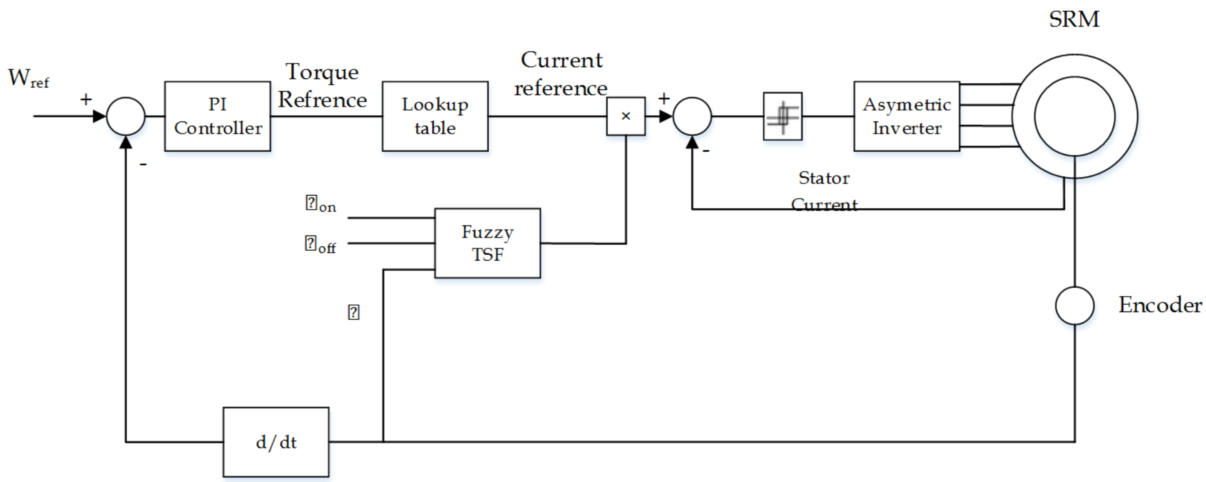

FIG. 9. Control structure.

overall torque function

$$\text{Torque function} = \begin{cases} \text{Rising FIS}, & \theta_1 < \theta < \theta_2 \\ (1 + k_1(\theta - \theta_3)^{k_2}), & \theta_2 < \theta < \theta_3 \\ \text{Falling FIS}, & \theta_3 < \theta < \theta_4 \end{cases} \quad (16)$$

where $_3$ is the turn off angel. Also, PSO has been used in parallel to the tuning of the FIS membership function to define k_1 and k_2. After optimization k_1 and k_2 is set to 0.13 and 3.14 respectively. Optimization objective function Eq. (17) is minimizing of the Torque Ripple (TR) Eq. (18):

$$OF = \int_0^t (\text{TR})^2 dt \quad (17)$$

$$\text{TR} = \left(\frac{T_{\max} - T_{\min}}{T_{av}}\right) \quad (18)$$

where TR is torque ripple and t is simulation time. The PSO population and iteration have considered 20 and 30, respectively. Objective function value during optimization process is shown in Fig. 10.

Input and output membership function of rising FIS after optimization are shown in Fig. 11 and 12, respectively, and for falling FIS is shown in Fig. 13 and 14, respectively.

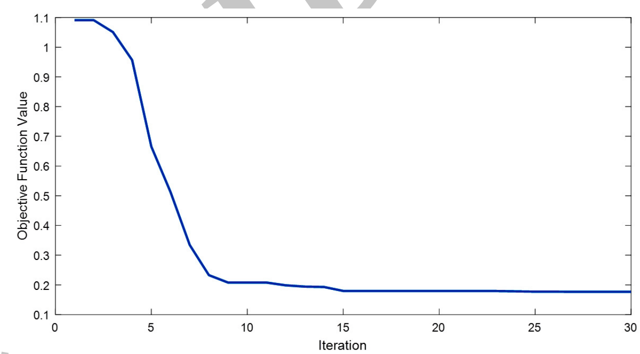

FIG. 10. Objective value during optimization period.

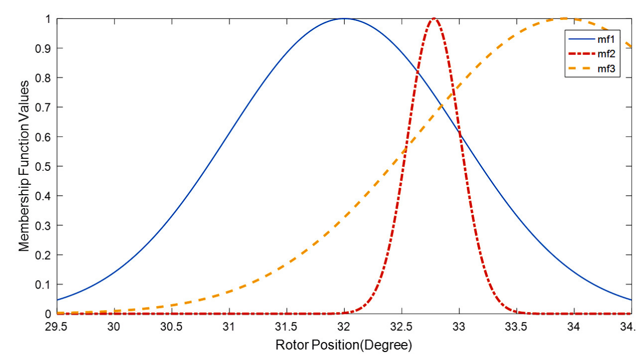

FIG. 11. Input membership function for rising FIS after optimization.

B. NUMERICAL STUDY AND RESULTS COMPARISON

To evaluate the effectiveness of the above mentioned method, this method has been compared with two methods. The first method is cosine TSF[17] and the second method is fuzzy TSF which has been proposed in[13]. The load torque is 1 Nm and the reference speed is 1000 rpm.

Fig. 15 shows that all of the three methods track the reference speed very well. Torque distribution of these three methods i.e. cosine TSF, Fuzzy TSF, and proposed Fuzzy PSO TSF are depicted in Fig. 16. Torque ripple (in pu) is shown in Fig. 17 for these three methods. Also, for a closer look, see Fig. 18.

To evaluate the proposed method, speed reference has been changed as 500, 1500, 2000, and 2500 rpm, respec-

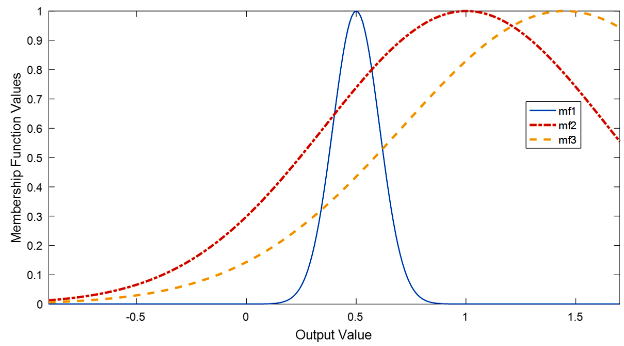

FIG. 12. Output membership function for rising FIS after optimization.

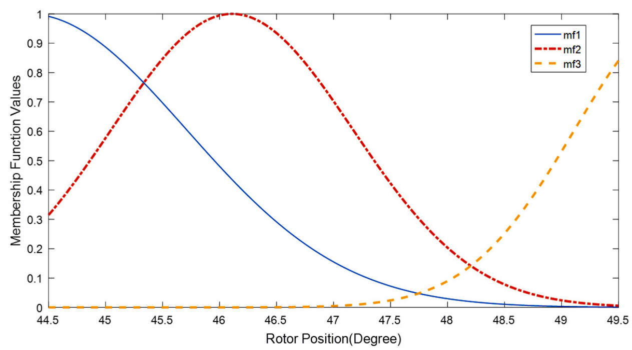

FIG. 13. Input membership function for falling FIS after optimization.

tively. Fig. 19 and Fig. 20 show speed tracking and ripple torque for the speed of 500. Also, for 1500 *rpm* speed tracking and ripple torque are shown in Fig. 21 and Fig. 22, respectively.

C. DISCUSSION

As can be seen in Fig. 15, speed tracking of these three methods are very well. There are differences in TSF of these three method. The first cosine TSF is smooth, but it makes a big torque ripple. The second method,

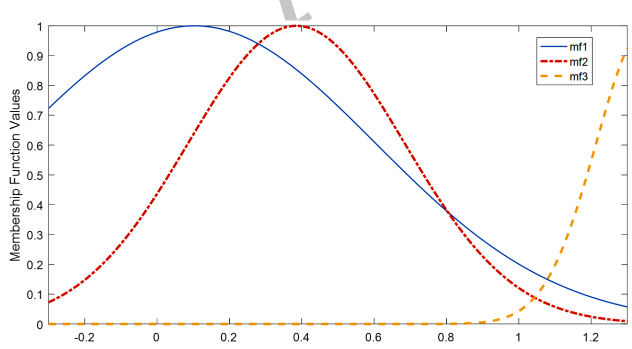

FIG. 14. Output membership function for falling FIS after optimization.

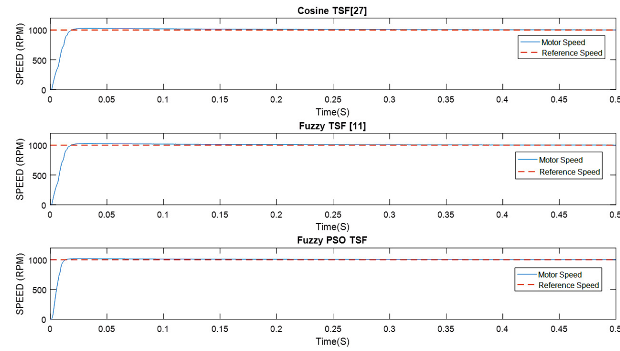

FIG. 15. Speed tracking of three methods.

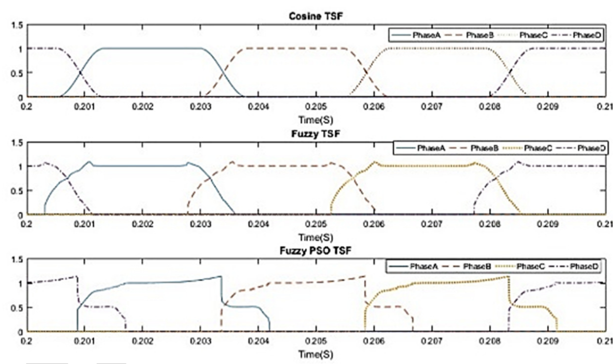

FIG. 16. Torque distribution (*pu*) shape in three TSFs.

i.e. fuzzy TSF, which is proposed in[13], is very good for three phase 12/8 SRM motor, but it makes large torque ripples when it comes to implementation for SRM with lower/higher poles (or simply for different SRM). For instance, the proposed fuzzy TSF does not result in a good torque as the poles of SRM decreased. As can be seen in Fig. 17 and Fig. 18, torque ripple of fuzzy TSF for four phase 8/6 is about 0.25 *pu* (or 25%), however it gives a better result for three phase 12/8 SRM.

The proposed method in this paper can result in a better answer since it enjoys two optimization algorithm

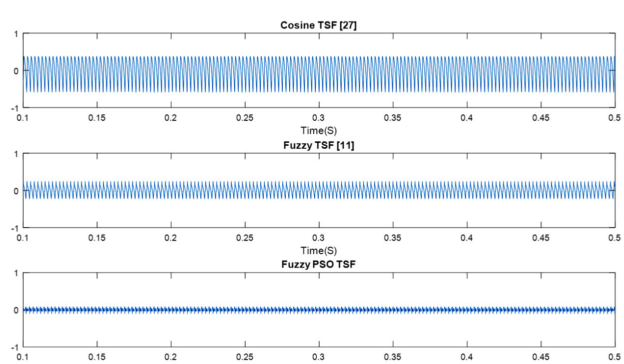

FIG. 17. Comparison of torque ripple (*pu*) in cosine, fuzzy, and fuzzy PSO TSF.

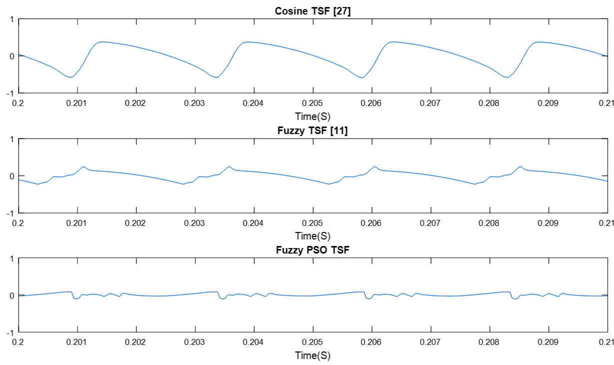

FIG. 18. Closer look to the torque ripple (pu) in cosine, fuzzy, and fuzzy PSO TSF.

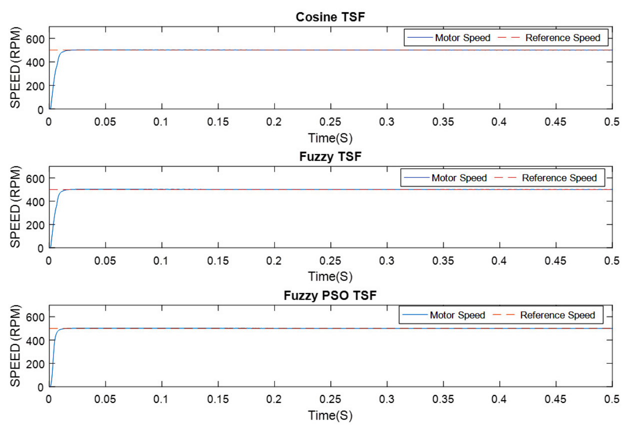

FIG. 19. Speed tracking of three methods for 500 rpm.

i.e. GA for starting and ending point of phase pulse and PSO for training fuzzy interface system. The proposed approach gives less than 0.07 pu (or 7%) torque ripple which is about one-third of the previous method. Also, it can be applied to any SRM, with any poles and phase and with any parameters. The proposed method can find the best TSF, since it enjoys two powerful optimization algorithm that can find the best TSF for any SRM. Moreover, in a closer look to Fig. 15, it can be seen that there is an increase in value of the torque reference in part in which a rotor pole is under a stator phase. The reason behind this is that, we are going to accelerate the rotor until compensate lack of the torque in commutation interval. This increase is given in Eq. (14). This feature can be considered as another tuning parameter which can improve torque response in different SRMs. Also, in Fig. 16, it is obvious that there is a phase shift in starting point of torque reference in the third method. This is because of GA has tuned the turn-on and turn-off angel as new values for the phase torque/current to reduce torque ripple. For a better comparison a criterion is defined as follows to compare the results:

$$C = 100 \times \int_{0.1}^{0.5} (\mathrm{TR})^2 dt \qquad (19)$$

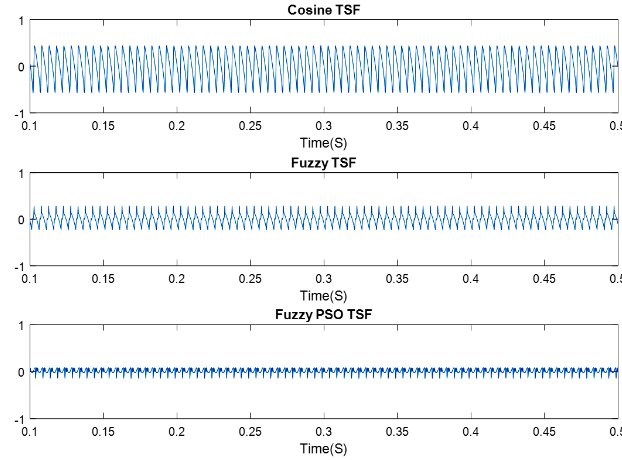

FIG. 20. Comparison of torque ripple (pu) in cosine, fuzzy, and fuzzy PSO TSF.

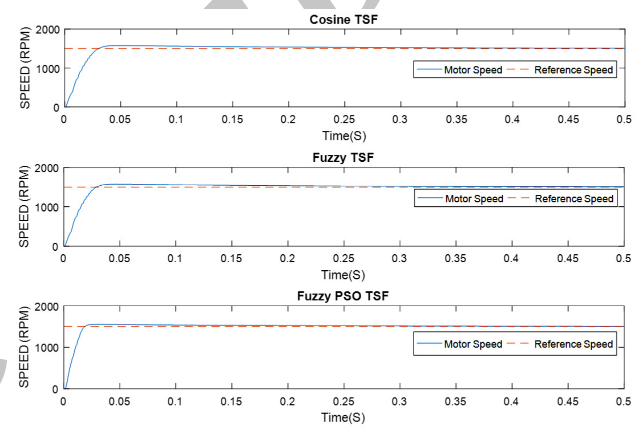

FIG. 21. Speed tracking of three methods 1500 rpm.

Which TR is torque ripple (in pu). This criterion for these three method is given in Table V. As can be seen, the proposed method improves torque ripple better than fuzzy TSF proposed in[13], and also better than Cosine TSF as proposed[17]. Criterion values for different speeds are given in Table V. It shows that the proposed fuzzy PSO gives lower torque ripple with any speed.

V. CONCLUSIONS

Due to the various merits of SRM, it has gained attention these days. The main drawback of the SRM is

TABLE V. Criterion value for three methods

Methods	Cosine TSF[17]	Fuzzy TSF[13]	Fuzzy PSO	Speed Reference
Criterion value	3.27	1.127	0.070	500 rpm
Criterion value	3.83	1.23	0.079	1000 rpm
Criterion value	3.94	1.857	0.099	1500 rpm

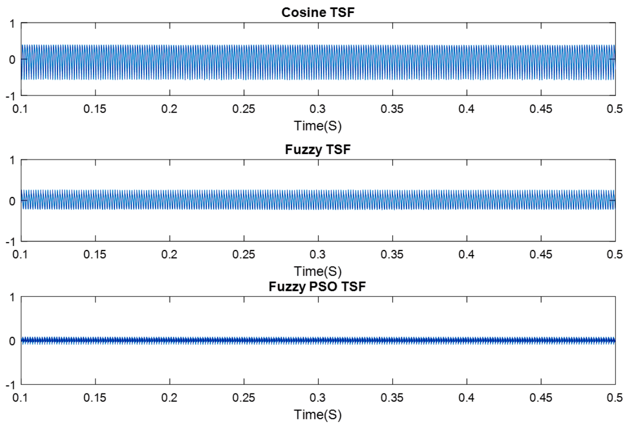

FIG. 22. Comparison of torque ripple (pu) in cosine, fuzzy, and fuzzy PSO TSF.

its big torque ripple which causes vibrations and sound noise. In this paper, two powerful optimization algorithm i.e. GA and PSO have been combined with intelligent fuzzy interface system to define rising and falling torque sharing function as well as the increase of the part in which cosine TSF and Fuzzy TSF have been considered constant. The effectiveness of this approach has been shown in a four phase 8/6 SRM, and the produced torque was high quality and its ripple was one-third of fuzzy TSF. This proposed method is very powerful to adapt itself for various kind of SRMs with different parameters.

APPENDIX

All variables and parameters used in this paper are given in Table VI.

TABLE VI. Variables and parameters

Variables and parameters	
v_k	$\mathrm{K^{th}}$ stator phase voltage
R_s	Stator phase resistance
λ_k	Linkage flux of $\mathrm{K^{th}}$ phase
θ_r	Rotor angle
i_k	$\mathrm{K^{th}}$ stator phase current
ω_r	Angular speed of the rotor
W_c	Co-energy
θ_i	Start angel of commutation interval
θ_f	Final angle of commutation interval
T_e	Sum of phase torques
T_k	Torques of $\mathrm{K^{th}}$ phase
T_x	X phase torques
T_y	Y phase torques
f_x	X TSF
f_y	Y TSF
M_F	Fuzzy Membership Function
T_R	Torque Ripple
PSO Variables	
X_i	$\mathrm{i^{th}}$ particle Position
G_B	Global best
P_B	Particle best
v_i	Particle velocity
w	Inertia weight
c_1 *and* c_2	Acceleration constants
r_1 *and* r_2	Random values in range $[0, 1]$
X	Position of particle

REFERENCES

[1] M. Tursini, M. Villani, G. Fabri and L. Di Leonardo, "A switched-reluctance motor for aerospace application: Design, analysis and results," *Electric Power Systems Research*, Vol. 142, pp. 74-83, 2017.
[2] X. Cao, Q. Sun, C. Liu, H. Zhou and Z. Deng, "Direct control of torque and levitation force for dual-winding bearingless switched reluctance motor," *Electric Power Systems Research*, Vol. 145, pp. 214-222, 2017.
[3] J. J. Wang, "A common sharing method for current and flux-linkage control of switched reluctance motor," *Electric Power Systems Research*, Vol. 131, pp. 19-30, 2016.
[4] Y. K. Choi, S. Y. Hee and S. K. Chang, "Pole-shape optimization of a switched-reluctance motor for torque ripple reduction," *IEEE Transactions on Magnetics*, Vol. 43, No. 4, pp. 1797-1800, 2007.
[5] S.I. Nabeta, I. E. Chabu, L. Luiz, D. A. P. Correa, W. M. Da Silva, and K. Hameyer, "Mitigation of the torque ripple of a switched reluctance motor through a multiobjective optimization," *IEEE Transactions on Magnetics* Vol. 44, No. 6, pp. 1018-1021, 2008.
[6] J. Ye, B. Berker and E. Ali, "An offline torque sharing function for torque ripple reduction in switched reluctance motor drives," *IEEE Transactions on Energy Conversion*, Vol. 30, No. 2, pp. 726-735, 2015.
[7] V. P. Vujicic, "Minimization of torque ripple and copper losses in switched reluctance drive," *IEEE transactions on power electronics*, Vol. 27, No. 1, pp. 388-399, 2012.
[8] D.H. Lee, L. Jianing, L. Zhen-Guo and A. Jin-Woo, "A simple nonlinear logical torque sharing function for low-torque ripple SR drive," *IEEE Transactions on Industrial Electronics*, Vol. 56, No. 8, pp. 3021-3028, 2009.
[9] S. K. Sahoo, S. K. Panda, and J. X. Xu, "Indirect torque control of switched reluctance motors using iterative learning control," *IEEE Transactions on Power Electronics*, Vol. 20, No. 1, p. pp. 200-208, Jan. 2005.
[10] S. K. Sahoo, S. K. Panda, and J. X. Xu, "Iterative learning-based high-performance current controller for switched reluctance motors," *IEEE Transactions on Energy Conversion*, Vol. 19, No. 3, pp. 491-498, 2004.
[11] A. Ghaheri, M. Milad and T. Hossein, "Sensorless Direct Torque Control Technique for Six-Phase Transverse Flux Permanent Magnet (TFPM) Motor," *PSC*, 2016.
[12] A. Siadatan, T. Hossein and A. Ebrahim, "Septi-segment switched reluctance machine: design, modeling, and manufacturing," *International Transactions on Electrical Energy Systems*, Vol. 26, No. 8, pp. 1673-1684, 2016.
[13] S. H. Ro, K. G. Lee, J. S. Lee, H. G. Jeong, and K. B. Lee, "Torque ripple minimization scheme using torque sharing function based fuzzy logic control for a switched reluctance motor," *Journal of Electrical Engineering & Technology*, Vol. 10, No. 1, pp. 118-127, 2015.
[14] M. Belhadi, K. Guillaume, M. Claude, H. Hala and M. Xavier, "Evaluation of axial SRM for electric vehicle application," *Electric Power Systems Research*, Vol. 148, pp. 155-161, 2017.
[15] P. Truong, D. Hoa, N. Flieller, N. Ky, M. Jean and S. Guy, "Torque ripple minimization in non-sinusoidal synchronous reluctance motors based on artificial neural networks," *Electric Power Systems Research*, Vol. 140, pp. 37-45, 2016.
[16] R. Krishnan, Switched reluctance motor drives: modeling, simulation, analysis, design, and applications, *CRC press*, 2001.

[17] R. S. Wallace and G. T. David, "A balanced commutator for switched reluctance motors to reduce torque ripple," *IEEE Transactions on Power Electronics*, Vol. 7, No. 4, pp. 617-626, 1992.
[18] A. M. Turing, "Computing machinery and intelligence-AM Turing," *Mind 59.236*, pp. 433-460, 1950.
[19] K. Hossein and D. Reza, "Comprehensive framework for capacitor placement in distribution networks from the perspective of distribution system management in a restructured environment," *International Journal of Electrical Power & Energy Systems*, Vol. 82, pp. 11-18, 2016.
[20] L. A. Zadeh, "Outline of a new approach to the analysis of complex systems and decision processes," *IEEE Transactions on systems, Man, and Cybernetics*, Vol. 1, pp. 28-44, 1973.
[21] E. Mamdani and S. Assilian, "An experiment in linguistic synthesis with a fuzzy logic controller," *International Journal of Man-Machine Studies*, Vol. 7, No. 1, pp. pp. 1-13, 1975.
[22] M. Sugeno, "Industrial applications of fuzzy control," *Elsevier Science Pub. Co.*, 1985.
[23] Webpage: Fuzzy Inference Systems.
[24] J. Kennedy, "Swarm intelligence," *In Handbook of nature-inspired and innovative computing, Springer, Boston, MA*, pp. 187-219, 2006.
[25] Z. Liu, C. Mao, J. Luo, Y. Zhang and C. L. P. Chen, "A three-domain fuzzy wavelet network filter using fuzzy PSO for robotic assisted minimally invasive surgery," *Knowledge-Based Systems*, Vol. 66, pp. 13-27, 2014.
[26] H. Karimi, B. T. H. Mohammad and R. Amin, "Decentralized voltage and frequency control in an autonomous ac microgrid using gain scheduling tuning approach," *Electrical Engineering (ICEE), 24th Iranian Conference on. IEEE*, 2016.
[27] K. L. Du and M. N. S. Swamy., "Particle swarm optimization," *Search and Optimization by Metaheuristics. Springer International Publishing*, pp. 153-173, 2016.
[28] S. K. Sahoo, S. K. Panda, and J. X. Xu, "Iterative learning-based high performance current controller for switched reluctance motors," *IEEE Transactions on Energy Conversion*, Vol. 19, No. 3, pp. 491-498, Sep. 2004.

Hassan Moradi CheshmehBeigi was born in Kermanshah, Iran, in 1979. He received his M.S. degree from the Faculty of Engineering, University of Shahid Beheshti, Tehran, Iran, in 2007. He received his Ph.D. degrees in Electrical Engineering from the Shahid Beheshti, Tehran, Iran, in 2011, respectively. In 2011, he joined the University of Razi, as an Assistant Professor in the Department of Electric Engineering. His current research interests Include Novel Electric Machine, Electric Machine Drives, Power Electronic Converters/Inverter.

Alireza Mohamadi Amidi was born in Kermanshah, Iran, in 1992. He received his M.S. degree from the Faculty of Engineering, University of Razi, Kermanshah, Iran, in 2017. His current research interests Include Electric Machine Drives and Power Electronic Converters.